

---

# ADROIT: A Self-Supervised Framework for Learning Robust Representations for Active Learning

Soumya Banerjee

*Department of Computer Science & Engineering  
IIT Kanpur*

*soumyab@cse.iitk.ac.in*

Vinay Kumar Verma

*Amazon, India*

*vinayugc@gmail.com*

## Abstract

Active learning aims to select optimal samples for labeling, minimizing annotation costs. This paper introduces a unified representation learning framework tailored for active learning with task awareness. It integrates diverse sources, comprising reconstruction, adversarial, self-supervised, knowledge-distillation, and classification losses into a unified VAE-based ADROIT approach. The proposed approach comprises three key components - a unified representation generator (VAE), a state discriminator, and a (proxy) task-learner or classifier. ADROIT learns a latent code using both labeled and unlabeled data, incorporating task-awareness by leveraging labeled data with the proxy classifier. Unlike previous approaches, the proxy classifier additionally employs a self-supervised loss on unlabeled data and utilizes knowledge distillation to align with the target task-learner. The state discriminator distinguishes between labeled and unlabeled data, facilitating the selection of informative unlabeled samples. The dynamic interaction between VAE and the state discriminator creates a competitive environment, with the VAE attempting to deceive the discriminator, while the state discriminator learns to differentiate between labeled and unlabeled inputs. Extensive evaluations on diverse datasets and ablation analysis affirm the effectiveness of the proposed model.

## 1 Introduction

Supervised deep learning (Krizhevsky et al., 2012) has achieved considerable success, particularly in terms of image recognition (He et al., 2016); however, the demand for extensive labeled datasets presents a formidable challenge (Ebrahimi et al., 2017). An alternative approach involves exploring various methods, such as self-supervised representation learning (Gidaris et al., 2018; Chen et al., 2020), active learning (Ren et al., 2021), and generative models (Kingma & Welling, 2013; Goodfellow et al., 2014; Luo, 2022; Kingma et al., 2021). These diverse methodologies serve distinct purposes; for example, obtaining good performance in self-supervised representation learning requires large amounts of unlabeled data. Generative models like VAEs (Kingma & Welling, 2013), GANs (Goodfellow et al., 2014), and diffusion models (Luo, 2022; Kingma et al., 2021) are typically aimed towards generative tasks rather than representation learning. Active learning focuses on acquiring functions to minimize the number of labeled samples. This study aims to investigate the question: Given access to an expensive labeling oracle, how can we effectively reduce the need for oracle access? While the active learning paradigm addresses this by learning acquisition functions, we propose a more holistic approach. Instead of solely learning an acquisition function, we suggest considering the entire datasets, both labeled and unlabeled with access to a labeling oracle to comprehensively utilize available information, ultimately minimizing the dependency on the labeling oracle.

Numerous active learning approaches, aimed at minimizing labeling costs by selecting informative samples from unlabeled pool (Ren et al., 2021), have been proposed. For instance, VAAL (Sinha et al., 2019) employs both labeled and unlabeled data to model input distributions, selecting informative unlabeled samples. Yet,

---

it is a task-agnostic approach, neglecting the conditional relation between input and output distributions. In contrast, models like TA-VAAL (Kim et al., 2021) and SRAAL (Zhang et al., 2020) incorporate class-conditional relationships, surpassing task-agnostic methods like VAAL (Sinha et al., 2019) and LL4AL (Yoo & Kweon, 2019). Despite these advancements, current methods under-utilize available unlabeled data for task learning (Gao et al., 2020; Huang et al., 2021; Cabannes et al., 2023), missing the opportunity to enhance visual representation and model performance (Chen et al., 2020). Self-supervised learning (Gidaris et al., 2018; Chen et al., 2020; Chen & He, 2021; Doersch et al., 2015; Noroozi & Favaro, 2016) exploits unlabeled data for intermediate representation learning, producing rich and semantically meaningful representations without requiring the knowledge of the annotation space (distribution). However, the integration of self-supervised learning into active learning remains under explored. Our objective is to investigate this integration not only for refining acquisition functions but also for improving the task-learner, unlocking the potential of unlabeled data for both model training and acquisition function learning.

This paper introduces a novel active learning (AL) method termed ***A** Self-Supervise**D** Framework for Learning **R**Obust Representat**I**ons for Ac**T**ive Learning* (ADROIT). This approach models the input distribution by leveraging both labeled and unlabeled data, integrating self-supervision to enhance representation learning from unlabeled samples. A unified representation learner (VAE) is employed (in the same spirit as VAAL (Sinha et al., 2019)), with an added adversarial network to identify the most informative unlabeled samples. Task-awareness is achieved through a proxy task-learner, minimizing cross-entropy loss on labeled data to explicitly capture the class-conditional dependence between annotation and input labeled data. The proxy learner also minimizes self-supervised rotation loss (SSL) on unlabeled data, enriching the latent-space representation, enhancing the performance of the proxy as well as the target task-learner, ultimately benefiting both model training and acquisition function learning. Additionally, a teacher-student learning approach is implemented between the target and proxy task-learner, ensuring emulation of the target learner’s behavior. Experimental results on diverse benchmark datasets, including balanced and imbalanced ones, demonstrate the superior performance of ADROIT over recent AL baselines. Extensive ablations further confirm the significance of the proposed components.

**Our contributions can be summarized as follows:**

- The proposed model integrates SSL to include both labeled and unlabeled data in the AL model.
- Utilizing a proxy task-learner or classifier, our model explicitly captures the conditional relationship between the output and input distribution. Additionally, it integrates the self-supervised rotation loss (SSL), making it an SSL-based task-aware AL approach.
- We employ teacher-student learning between the target and proxy task learner. It enforces the proxy classifier to imitate the behavior of the target model while simultaneously capturing the conditional dependence and minimizing SSL.
- Empirical evaluations and ablations on diverse datasets with varying class balances validate the superiority of ADROIT over existing baselines.

## 2 Method

### 2.1 Overview

This section outlines the active learning (AL) setup and introduces the notation for the paper. In AL, there’s a target task (e.g., image classification) and a task-learner ( $T$ ) parameterized by  $\zeta$ . Initially, a large unlabeled pool  $X_U$  exists, from which  $M$  samples are randomly labeled by an oracle, forming the labeled pool  $(X_L, Y)$ . Each AL iteration selects a subset of samples with a budget ( $b$ ) from  $X_U$  using an acquisition function and annotates them. Therefore, the labeled pool grows in size with each iteration, whereas the unlabeled pool shrinks. The task-learner ( $T$ ) is trained in each AL cycle, by minimizing the sum of cross-entropy loss on labeled data and self-supervised rotation-loss (Gidaris et al., 2018) on unlabeled data. Algorithm 3 illustrates the various steps of training the target task-learner ( $T_\zeta$ ) in each stage of active learning.

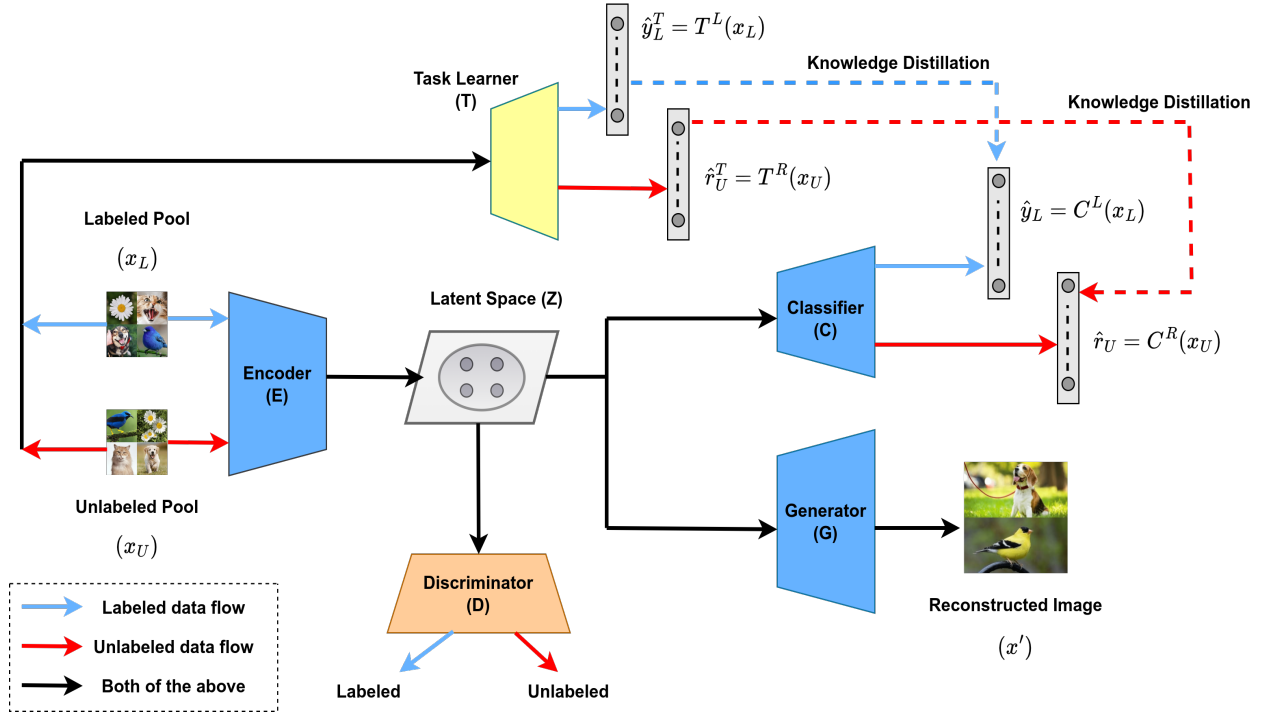


Figure 1: The proposed framework, named *A Self-Supervised Framework for Learning Robust Representations for Active Learning* (ADROIT), comprises a unified representation generator (VAE) with an encoder ( $E$ ) and a generator network ( $G$ ), a classifier network ( $C$ ), and a state discriminator ( $D$ ). The VAE learns a unified latent space using both labeled and unlabeled data. The classifier network incorporates annotation information into the latent space and refines it through self-supervised loss optimization with unlabeled data. Teacher-student training aligns the classifier ( $C$ ) with the target task-learner ( $T$ ). Meanwhile, the state discriminator distinguishes between labeled and unlabeled samples, aiding in the selection of informative unlabeled samples.

The proposed framework, *A Self-Supervised Framework for Learning Robust Representations for Active Learning* (ADROIT), is illustrated in Figure 1. The subsequent sections provide detailed descriptions of the different components of ADROIT.

## 2.2 Unified Representation Learning

In this work, we employ a  $\beta$ -variational autoencoder ( $\beta$ -VAE) (Kingma & Welling, 2013; Weng, 2018) to learn a unified latent-space representation from both labeled and unlabeled data. The encoder network ( $E$ ), with parameters  $\phi$ , learns a latent-space representation for the underlying data distribution using a Gaussian prior on the latent code, and the generator network ( $G$ ), with parameters  $\xi$ , reconstructs the input data from the latent code. As labeled and unlabeled data share the same distribution  $\mathcal{X}$ , the VAE learns the latent representation using both of them and is optimized by minimizing the variational lower bound. The objective function for the  $\beta$ -VAE is formulated as:

$$\mathcal{L}_{\text{VAE}}^{\text{URL}} = \mathbb{E} [\log G_{\xi}(x_L|z_L)] - \beta \text{D}_{\text{KL}}(E_{\phi}(z_L|x_L) || p(z)) + \mathbb{E} [\log G_{\xi}(x_U|z_U)] - \beta \text{D}_{\text{KL}}(E_{\phi}(z_U|x_U) || p(z)) \quad (1)$$

where  $E_{\phi}(\cdot)$  and  $G_{\xi}(\cdot)$  denotes the encoder ( $E$ ) and the generator ( $G$ ) network, parameterized by  $\phi$  and  $\xi$ , respectively,  $p(z)$  is the prior chosen as the Gaussian unit, and  $\beta$  is a hyperparameter to control the trade-off between reconstruction ability and regularization of the latent space.

---

### 2.3 Class Conditional and Self-supervised Representation Learning

In the unified representation learning step (Section 2.2), the model captures the input distribution from both labeled and unlabeled data. However, it does not take into account the conditional dependence between inputs and labels. To address this, we introduce a proxy task-learner, mimicking the actual task-learner ( $T$ ), to incorporate these conditional dependencies into the learning of the latent space.

The proxy task-learner ( $C$ ), with parameters  $\Psi$ , serves two purposes. Firstly, it predicts the class labels for the labeled inputs using their latent codes. Secondly, it predicts the rotations applied to unlabeled inputs using their latent codes. It minimizes cross-entropy loss on labeled data and self-supervised rotation-loss (SSL) (Gidaris et al., 2018) on unlabeled data. This approach explicitly integrates conditional dependence between the inputs and annotations into the latent space while refining the latent representation through SSL. We apply one of six random transformations on unlabeled data and enforces the proxy task-learner to accurately predict the applied transformation: (i)  $0^\circ$  rotation, (ii)  $90^\circ$  rotation, (iii)  $180^\circ$  rotation, (iv)  $270^\circ$  rotation, (v) horizontal-flip, and (vi) vertical-flip.

The objective functions for supervised and self-supervised learning are formulated as:

$$\mathcal{L}_C^L = \mathbb{E} [\log C_\Psi^L(y_L|z_L)] - \text{D}_{\text{KL}}(E_\phi(z_L|x_L) || p(z)) \quad (2)$$

$$\mathcal{L}_C^U = \mathbb{E} [\log C_\Psi^R(r_U|z_U)] - \text{D}_{\text{KL}}(E_\phi(z_U|x_U) || p(z)) \quad (3)$$

where  $z_L$  and  $z_U$  denote the latent variable from the latent space for labeled and unlabeled data respectively,  $C_\Psi(\cdot)$  denotes the proxy task-learner ( $C$ ), with parameters  $\Psi$ , and  $C_\Psi^L(\cdot)$  and  $C_\Psi^R(\cdot)$  denotes the labeled and rotation head respectively.

### 2.4 Teacher-Student Learning

The proxy task-learner ( $C$ ) aims to mimic the target task-learner ( $T$ ). Still, it might not accurately replicate how the task-learner estimates the conditional dependence  $p(y|x)$  using labeled data. Moreover, the proxy task-learner may learn distinct visual features from those of the task-learner. To align their behavior, we establish teacher-student learning between the target and proxy task-learners, employing knowledge-distillation loss (Hinton et al., 2015) where the target task-learner acts as the teacher network. This process involves minimizing the mean-squared error between the corresponding logits generated by the target and proxy task-learner. The target task-learner remains unchanged during this optimization, with only the proxy task-learner being updated.

The objective function for teacher-student learning is formulated as:

$$\mathcal{L}_{\text{KD}} = \mathbb{E}_{x_L \sim X_L} [\|T_\zeta^L(x_L) - C_\Psi^L(E_\phi(x_L))\|_2^2] + \mathbb{E}_{x_U \sim X_U} [\|T_\zeta^R(x_U) - C_\Psi^R(E_\phi(x_U))\|_2^2] \quad (4)$$

where  $X_L$  and  $X_U$  denote labeled and unlabeled data pool respectively,  $E_\phi(\cdot)$  denote the encoder network,  $C_\Psi(\cdot)$  and  $T_\psi(\cdot)$  represents proxy and target task-learner respectively, and  $T_\zeta^L(\cdot)$  and  $T_\zeta^R(\cdot)$  denote the labeled and rotation head, respectively.

### 2.5 Adversarial Representation Learning

The VAE’s latent space integrates both labeled and unlabeled data, capturing input distribution  $p(x)$  and conditional dependence  $p(y|x)$ . Our objective is to leverage these representations for identifying informative samples from the unlabeled pool. We achieve this by training an adversarial network on the VAE’s latent space, akin to a GANs’ discriminator (Goodfellow et al., 2014). It discerns labeled and unlabeled latent codes (treating it as a classification problem where the labeled inputs are class 1 and unlabeled inputs are class 0), effectively categorizing the latent space into these two groups. Once trained, the adversarial network

---

**Algorithm 1** ADROIT

---

**Require:** Labeled pool  $(X_L, Y)$ , Unlabeled pool  $(X_U)$

**Require:** Trained task-learner  $T_\zeta(\cdot)$   $\triangleright$  it is kept frozen while training the VAE and the state-discriminator

**Require:** Initialize model parameters:  $\Theta_{\text{VAE}}$ , and  $\theta_D$   $\triangleright \Theta_{\text{VAE}}$  represents the parameters of the whole VAE network including Encoder ( $E$ ), Generator ( $G$ ), & Classifier ( $C$ ), and  $\theta_D$  represents the parameters of the state-discriminator ( $D$ )

**Require:** Hyper-parameters: epochs,  $\lambda_1, \lambda_2, \lambda_3, \lambda_4, \alpha_1$ , and  $\alpha_2$

```
1: for  $e = 1$  to epochs do
2:   sample  $(x_L, y) \sim (X_L, Y)$  and  $x_U \sim X_U$ 
3:   Compute  $\mathcal{L}_{\text{VAE}}^{\text{URL}}$  by using Eq. (1)
4:   Compute  $\mathcal{L}_C^L$  by using Eq. (2)
5:   Compute  $\mathcal{L}_C^U$  by using Eq. (3)
6:   Compute  $\mathcal{L}_{\text{KD}}$  by using Eq. (4)
7:   Compute  $\mathcal{L}_{\text{VAE}}^{\text{adv}}$  by using Eq. (5)
8:    $\mathcal{L}_{\text{VAE}} \leftarrow \mathcal{L}_{\text{VAE}}^{\text{URL}} + \lambda_1 \mathcal{L}_C^L + \lambda_2 \mathcal{L}_C^U + \lambda_3 \mathcal{L}_{\text{KD}} + \lambda_4 \mathcal{L}_{\text{VAE}}^{\text{adv}}$ 
9:   Update VAE by descending its stochastic gradients:
10:   $\Theta_{\text{VAE}}' \leftarrow \Theta_{\text{VAE}} - \alpha_1 \nabla \mathcal{L}_{\text{VAE}}$ 
11:  Compute  $\mathcal{L}_D$  by using Eq. (6)
12:  Update  $D$  by descending its stochastic gradients:
13:   $\theta_D' \leftarrow \theta_D - \alpha_2 \nabla \mathcal{L}_D$ 
14: end for
15: return Trained  $\Theta_{\text{VAE}}$ , and  $\theta_D$ 
```

---

assists in selecting informative unlabeled samples: unlabeled inputs that “look like” labeled inputs, i.e., high probability of belonging to class 1, are discarded, and (a subset of the) others are chosen for annotation by the oracle (using a scheme in Section 2.6).

The VAE and adversarial network are jointly trained adversarially, similar to GANs (Goodfellow et al., 2014). The VAE emulates the generator, aiming to mislead the adversarial network into classifying both labeled and unlabeled inputs as 1. Conversely, the adversarial network correctly classify latent representations as labeled (class 1) or unlabeled (class 0), distinguishing between samples from the labeled pool  $X_L$  and the unlabeled pool  $X_U$ .

The objective function for VAE as the generator network is formulated as the binary cross-entropy loss as:

$$\mathcal{L}_{\text{VAE}}^{\text{adv}} = -\mathbb{E} [\log D_\theta(E_\phi(z_L|x_L))] - \mathbb{E} [\log D_\theta(E_\phi(z_U|x_U))] \quad (5)$$

where  $D_\theta(\cdot)$  represents the adversarial discriminator network ( $D$ ), parameterized by  $\theta$ .

The objective function for adversarial learning of the discriminator is formulated as:

$$\mathcal{L}_D = -\mathbb{E} [\log D_\theta(E_\phi(z_L|x_L))] - \mathbb{E} [\log(1 - D_\theta(E_\phi(z_U|x_U)))] \quad (6)$$

The total objective function for the VAE is obtained by combining Eq. (1), Eq. (2), Eq. (3), Eq. (4) and Eq. (5), as follows:

$$\mathcal{L}_{\text{VAE}} = \mathcal{L}_{\text{VAE}}^{\text{URL}} + \lambda_1 \mathcal{L}_C^L + \lambda_2 \mathcal{L}_C^U + \lambda_3 \mathcal{L}_{\text{KD}} + \lambda_4 \mathcal{L}_{\text{VAE}}^{\text{adv}} \quad (7)$$

where  $\lambda_1, \lambda_2, \lambda_3$  and  $\lambda_4$  are hyperparameters that determine the effect of various components to learn an effective latent-space representation.

Algorithm 1 shows various steps of the proposed model.

---

**Algorithm 2** Sampling Strategy

---

**Require:**  $(X_L, Y)$ , and  $X_U$ **Require:** Trained models:  $\Theta_{\text{VAE}}$  and  $\theta_D$   $\triangleright \Theta_{\text{VAE}}$  denotes the parameters of the whole VAE and  $\theta_D$  denotes the parameters of the state-discriminator ( $D$ )**Require:** Sampling budget:  $b$ 

- 1: Select samples  $(X_s)$  with  $\min_b \{D_{\theta}(E_{\phi}(z_U|x_U))\}$
  - 2:  $Y_o \leftarrow \text{ORACLE}(X_s)$
  - 3:  $(X_L, Y) \leftarrow (X_L, Y) \cup (X_s, Y_o)$
  - 4:  $X_U \leftarrow X_U - X_s$
  - 5: **return**  $(X_L, Y)$  and  $X_U$
- 

**Algorithm 3** Target Task-Learner Training

---

**Require:**  $(X_L, Y)$ , and  $X_U$ **Require:** Target Task-learner:  $T_{\zeta}(\cdot)$ **Require:** Initialize model parameters:  $\zeta_T$   $\triangleright \zeta_T$  denotes the parameters of the target task-learner ( $T$ )**Require:** Hyper-parameters: epochs,  $\eta$ ,  $\xi$ 

- 1: **for**  $e = 1$  to epochs **do**
  - 2:   sample  $(x_L, y) \sim (X_L, Y)$  and  $x_U \sim X_U$
  - 3:    $\mathcal{L}_T^L = \mathcal{L}_{CE}(y, T_{\zeta}^L(x_L))$   $\triangleright \mathcal{L}_{CE}(\cdot, \cdot)$  denotes cross-entropy loss and  $T_{\zeta}^L(\cdot)$  represents that the label-prediction head is used to generate output
  - 4:    $\mathcal{L}_T^U = \mathcal{L}_{CE}(r_U, T_{\zeta}^R(x_U))$   $\triangleright T_{\zeta}^R(\cdot)$  represents that the rotation-prediction head is used to generate output
  - 5:    $\mathcal{L} = \mathcal{L}_T^L + \xi \mathcal{L}_T^U$
  - 6:   Evaluate  $\nabla_{\zeta} \mathcal{L}(T_{\zeta})$
  - 7:   Update task-learner ( $T$ ) by descending its stochastic gradients:
  - 8:    $\zeta'_T = \zeta_T - \eta \nabla_{\zeta} \mathcal{L}(T_{\zeta})$
  - 9: **end for**
  - 10: **return** Trained Task-learner  $T_{\zeta}(\cdot)$
- 

## 2.6 Sampling Strategy

After training ADROIT, the data-points  $(x_U^1, \dots, x_U^b)$  to be labeled at each iteration are selected as:

$$(x_U^1, \dots, x_U^b) = \arg \min_{(x_U^1, \dots, x_U^b) \subset X_U} D_{\theta}(E_{\phi}(z_U|x_U)) \quad (8)$$

The details of sample selection is shown in the Algorithm 2.

## 3 Related Work

### 3.1 Active Learning

Active Learning (AL) (Ren et al., 2021; Sinha et al., 2019; Kim et al., 2021; Mottaghi & Yeung, 2019; Zhang et al., 2020; Guo et al., 2021; Wang et al., 2020; Shui et al., 2020; Li et al., 2021b; Jin et al., 2022; Ebrahimi et al., 2020; Sener & Savarese, 2017; Agarwal et al., 2020; Geifman & El-Yaniv, 2019; Gal et al., 2017; Kirsch et al., 2019; Yoo & Kweon, 2019; Zhan et al., 2022) strategies aim to choose the most informative samples from an unlabeled pool for labeling by an oracle. Recent works have proposed various AL methods, which broadly can be categorized into (i) task-agnostic and (ii) task-aware approaches, depending on whether the AL sample selection strategy explicitly considers the conditional relationship between the output and input distribution. Moreover, existing AL techniques can also be grouped into (i) uncertainty-based and (ii) diversity-based approaches. Some AL methods are also characterized as query-by-committee-based approaches. The following provides a brief overview of these diverse AL approaches.

---

### 3.1.1 Task-agnostic and Task-aware AL approaches

Task-agnostic approaches (Sinha et al., 2019; Ren et al., 2021; Zhu & Bento, 2017; Yoo & Kweon, 2019) model the input data distribution without considering the conditional relationship between input and output. VAAL (Sinha et al., 2019) models the input distribution by employing data from both the labeled and unlabeled pools through a VAE (Kingma & Welling, 2013). The VAE captures a low-dimensional latent space representation, which is subsequently used to train an adversarial network (Goodfellow et al., 2014). Once trained, this adversarial network identifies the most informative samples. Another example is GAAL (Zhu & Bento, 2017), which generates adversarial samples causing high uncertainty in the learner. These samples are then labeled by an oracle and integrated into the labeled pool. Similarly, LL4AL (Yoo & Kweon, 2019) learns to predict target losses for unlabeled inputs and selects unlabeled samples with the top-k losses for labeling and inclusion in the labeled pool. In contrast, task-aware methods (Ren et al., 2021; Kim et al., 2021; Zhang et al., 2020) explicitly leverage conditional dependence through task-specific modeling. SRAAL (Zhang et al., 2020), an extension of VAAL (Sinha et al., 2019), introduces an uncertainty indicator for unlabeled samples, assigning them different levels of importance. TA-VAAL (Kim et al., 2021) incorporates a ranking-loss framework (Yoo & Kweon, 2019; Saquil et al., 2018) into the VAE structure. Both SRAAL (Zhang et al., 2020) and TA-VAAL (Kim et al., 2021) employ an adversarial network to identify the top-k unlabeled samples.

### 3.1.2 Uncertainty and Diversity based AL approaches

The distinction between uncertainty-based and diversity-based AL approaches lies in their selection of unlabeled samples. Uncertainty-based strategies, like BALD (Gal et al., 2017) and MC-Dropout (Houlsby et al., 2011), target samples where the model is uncertain, using this uncertainty as an indicator of potential model errors. In contrast, diversity-based approaches, such as Coreset (Sener & Savarese, 2017), aim to maximize diversity within the selected samples. For example, BALD maximizes mutual information between model predictions and parameters, while Coreset employs a greedy  $K$ -center algorithm for diverse sample selection. Additionally, DAAL (Wang et al., 2020) utilizes two adversarial networks, with one estimating uncertainty and the other maximizing the diversity of chosen samples.

### 3.1.3 Query-By-Committee based AL approaches

“Query-By-Committee” based AL approaches, also referred to as agreement-based AL methods, diverge from the conventional AL approaches by utilizing an ensemble of diverse models to gauge the uncertainty of a sample from the unlabeled pool rather than relying on a single model (Beluch et al., 2018; Cohn et al., 1994; Cortes et al., 2019; Iglesias et al., 2011; McCallum et al., 1998; Seung et al., 1992; Gao et al., 2020). For a sample, if the predictions across the ensemble of models vary largely then this sample is considered most uncertain sample. Therefore, it is selected for labeling.

## 3.2 Self-supervised Learning

Self-supervised learning (SSL)(Gidaris et al., 2018; Chen et al., 2020; Mishra et al., 2022; He et al., 2022; Chen & He, 2021; Caron et al., 2021; Li et al., 2021a; Weng, 2019; Balestrieri et al., 2023) aims to train deep neural networks (DNNs) using almost freely available vast amounts of unlabeled data by defining a pretext task based on the data itself. This allows the model to learn rich, descriptive, and generic representations for downstream tasks. In this paper, we applied six different random transformations uniformly to the unlabeled samples and enforced the network to predict the applied transformation as a pretext task. This approach aims to learn robust visual features using the freely available, abundant pool of unlabeled data (refer to Section 2.3).

## 3.3 Variational AutoEncoder

Autoencoders (Hinton & Salakhutdinov, 2006; Hinton et al., 2011) have long been used for representation learning and dimensionality reduction. They comprise two networks: an encoder, which maps input data to a latent space, and a decoder, which generates input data from the latent code. These networks learn identity

---

mapping in an unsupervised manner by minimizing reconstruction errors. The Variational Autoencoder (VAE) (Kingma & Welling, 2013; Weng, 2018; Doersch, 2016) is also a latent variable model that follows a similar encoder-decoder architecture. However, a VAE’s encoder network maps each high-dimensional input data to a latent distribution using a Gaussian prior for the latent code. The decoder then reconstructs the input data from this latent distribution. Once trained, the decoder can operate independently to generate new synthetic data. Recently, a lot of research has exploited VAE-like architectures in various applications, ranging across generative modeling (Kingma & Welling, 2013; Chen et al., 2016b; Kingma et al., 2021; 2016; Vahdat & Kautz, 2020; Razavi et al., 2019; Yan et al., 2021), anomaly detection (Xu et al., 2018), semi-supervised learning (Kingma et al., 2014), sequence-to-sequence modeling (Kaiser et al., 2018; Bahuleyan et al., 2017), and active learning (Sinha et al., 2019; Ren et al., 2021). In this paper, we use a VAE-like architecture to learn a unified latent representation by exploiting both labeled and unlabeled data at each stage of active learning (refer to Section 2.2).

### 3.4 Adversarial Learning

The Generative Adversarial Network (GAN)(Goodfellow et al., 2014) comprises two networks: (i) a generator network that learns to create realistic data from a latent Gaussian distribution, and (ii) a discriminator network that learns to accurately differentiate between the generated (fake) samples and real data. Adversarial learning has been extensively used in various domains, including generative modeling(Goodfellow et al., 2014; Radford et al., 2015; Mirza & Osindero, 2014; Wang et al., 2022), image-to-image translation (Zhu et al., 2017a; Lin et al., 2018; Isola et al., 2017; Ma et al., 2018), domain generalization (Ganin & Lempitsky, 2015; Zhang et al., 2022; Huang et al., 2018), data augmentation (Antoniou et al., 2017; Zhu et al., 2017b; Calimeri et al., 2017), representation learning (Chen et al., 2016a; Donahue et al., 2017; Huang et al., 2017; Odena, 2016; Donahue et al., 2016), and active learning (Sinha et al., 2019; Ren et al., 2021). In this paper, we also exploit adversarial learning to determine the most informative unlabeled samples for annotation at each stage of active learning (refer to Section 2.5).

## 4 Experiments

We conduct extensive experiments to demonstrate the effectiveness of our proposed approach. For a robust evaluation, we evaluate our approach on class-balanced as well as class-imbalanced datasets.

### 4.1 Active Learning on Balanced Datasets

**Balanced benchmark datasets.** We evaluate the proposed AL model (ADROIT) on four balanced benchmark datasets: CIFAR10/100 (Krizhevsky et al., 2009), TinyImageNet-200 (Le & Yang, 2015) and ImageNet-100 (a subset of ImageNet-1K (Deng et al., 2009)). Initially, 1000 and 2000 samples are randomly labeled for CIFAR10/100 and TinyImageNet-200/ImageNet-100. In subsequent iterations, 1000 and 2000 samples are selected through active learning strategies and annotated by an oracle. We provide more details in the appendix.

**Compared methods.** We compare the performance of our method (ADROIT) with recent state-of-the-art baselines, including VAAL (Sinha et al., 2019), MC-Dropout (Gal et al., 2017), Coreset (Sener & Savarese, 2017), LL4AL (Yoo & Kweon, 2019), SRAAL (Zhang et al., 2020), and TA-VAAL (Kim et al., 2021). Random sample selection is also included for comparison. All methods are trained from scratch using original code and hyperparameters, and evaluation employs the same target learner.

**Implementation details.** We use ResNet-18 (He et al., 2016) as the target task-learner for ImageNet-100, along with adapting it for CIFAR10/100 and TinyImageNet-200, with SGD optimizer (lr: 0.01, momentum: 0.9, weight decay: 0.005). The VAE employs a modified Wasserstein autoencoder (Tolstikhin et al., 2017) with a 5-layer MLP discriminator, similar to VAAL (Sinha et al., 2019) and TA-VAAL (Kim et al., 2021). Both the VAE and discriminator use the Adam optimizer (Kingma & Ba, 2014) (lr:  $5 \times 10^{-4}$ ). For more details, please refer to the appendix.

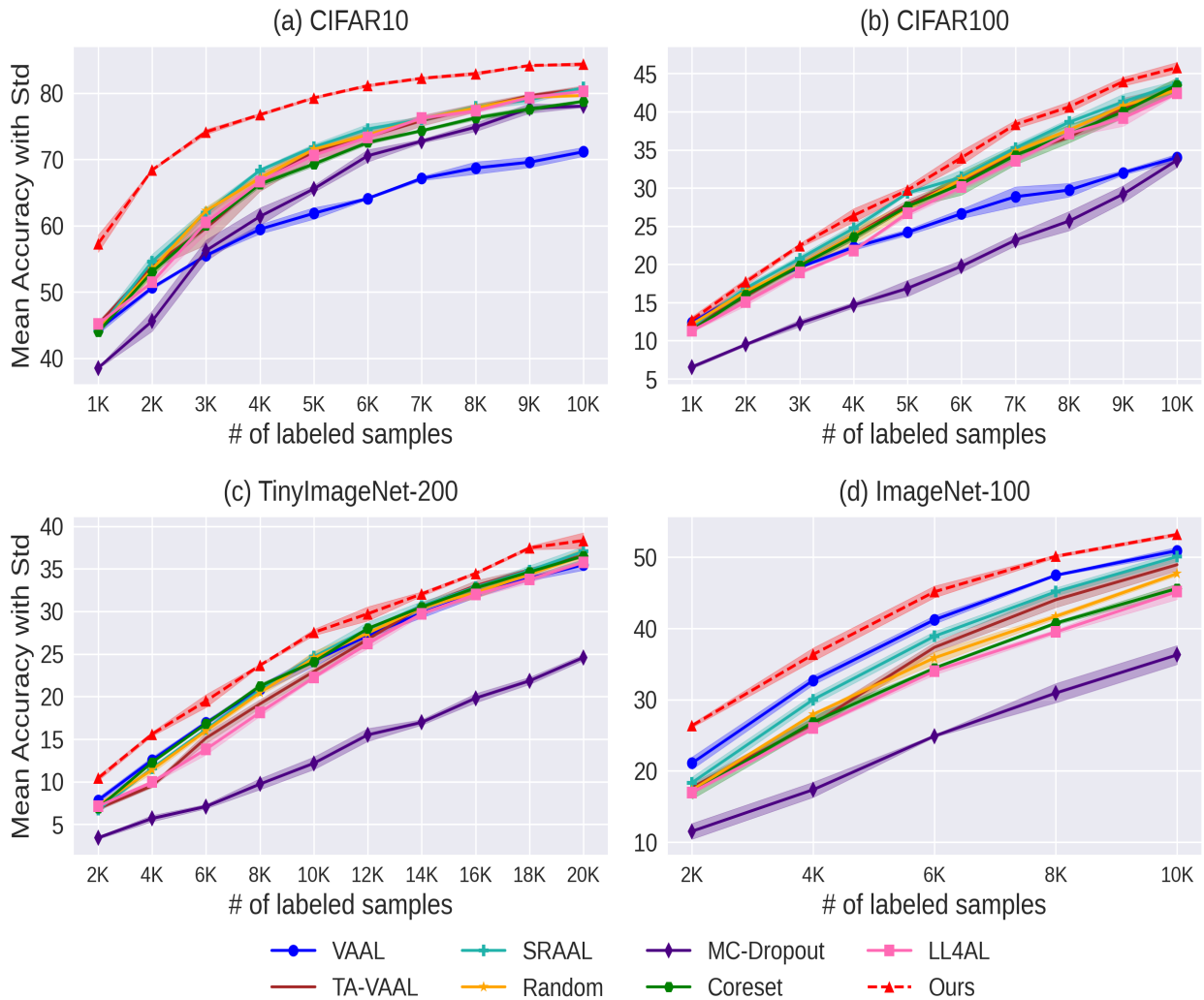


Figure 2: Mean accuracy with standard deviations (shaded) of AL methods over the number of labeled samples on CIFAR10/100 (balanced), TinyImageNet-200 (balanced) and ImageNet-100 (balanced).

**Performance on CIFAR10.** In Figure 2(a), we present the performance of active learning (AL) methods, including ADROIT, on the CIFAR10 dataset. Notably, ADROIT outperforms all other baseline methods, with SRAAL ranking as the second-best performing AL baseline. Initially, for smaller sample sizes, VAAL achieves comparable accuracy to other baseline methods but experiences a decline in performance in subsequent iterations, ultimately falling behind all other methods in comparison. MC-Dropout initially lags behind all other methods, but by the third iteration, it surpasses VAAL and achieves accuracy levels similar to Coreset. In summary, ADROIT exhibits a substantial 8.13% higher mean accuracy compared to the best-performing baseline.

**Performance on CIFAR100.** We next present the results on the more challenging CIFAR100 dataset. In Figure 2(b), we present the empirical performance of active learning (AL) methods, including ADROIT, on CIFAR100. It’s apparent that ADROIT emerges as the top performer, outperforming all other baselines by a significant margin. The recent approach, SRAAL, takes second place, although Coreset and LL4AL exhibit highly competitive results compared to SRAAL. In the final iteration, both MC-Dropout and VAAL achieve similar accuracy but lag behind all other compared baselines. Overall, ADROIT demonstrates a 1.79% absolute improvement over the second-best-performing method, SRAAL.

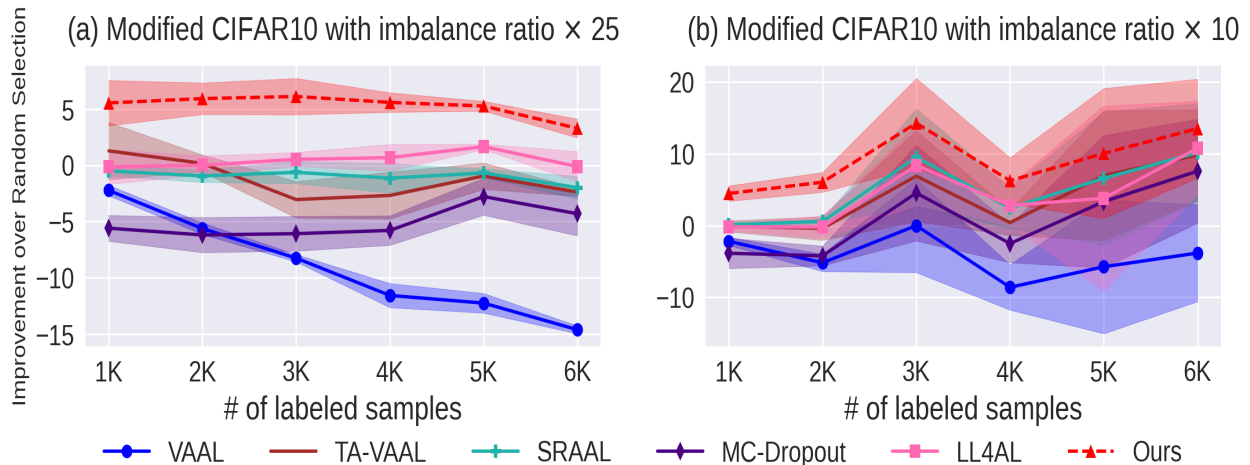


Figure 3: Mean accuracy improvements with standard deviations (shaded) of AL methods w.r.t random sampling over the number of labeled samples on modified imbalanced CIFAR10 dataset.

**Performance on TinyImageNet-200.** TinyImageNet-200, a subset of ImageNet-1K (Deng et al., 2009), presents a more challenging task than CIFAR10/100. In Figure 2(c), we observe the empirical performance of the compared baselines. Notably, ADROIT outperforms all previous baselines, establishing its efficacy on this challenging dataset. In this setting too, SRAAL is the best performer in the baseline methods. Remarkably, VAAL attains better accuracy on TinyImageNet-200 compared to CIFAR10/100. VAAL even initially ranks as the second-best-performing AL method. Random sampling initially outperforms LL4AL and TA-VAAL but eventually converges to a similar level of performance as these methods. MC-Dropout consistently performs the worst among all baselines. Overall, ADROIT achieves a performance gain of 2.6% with respect to SRAAL, showing the efficacy of the proposed model over the highly challenging dataset.

#### Performance on ImageNet-100.

ImageNet-100 is a subset of ImageNet-1K (Deng et al., 2009), wherein the subset’s classes are randomly selected. Detailed information about the 100 classes is available in the appendix. Figure 2(d) demonstrates the empirical performances of various active learning (AL) approaches, including ADROIT. Notably, ADROIT consistently outperforms all other baselines throughout the AL iterations, achieving a 3.6% performance gain compared to the second-best AL method, VAAL. Remarkably, SRAAL underperforms compared to VAAL but outperforms other baselines. In the initial AL iterations, the other baselines (excluding MC-Dropout) achieve similar accuracy, but by the third iteration, TA-VAAL surpasses them, ultimately performing similarly to SRAAL. MC-Dropout, in contrast to other baselines, including ADROIT, exhibits the worst performance throughout the AL iterations on ImageNet-100. In summary, ADROIT emerges as the top-performing AL method on ImageNet-100, a subset of ImageNet-1K, with an overall 3.6% higher mean accuracy.

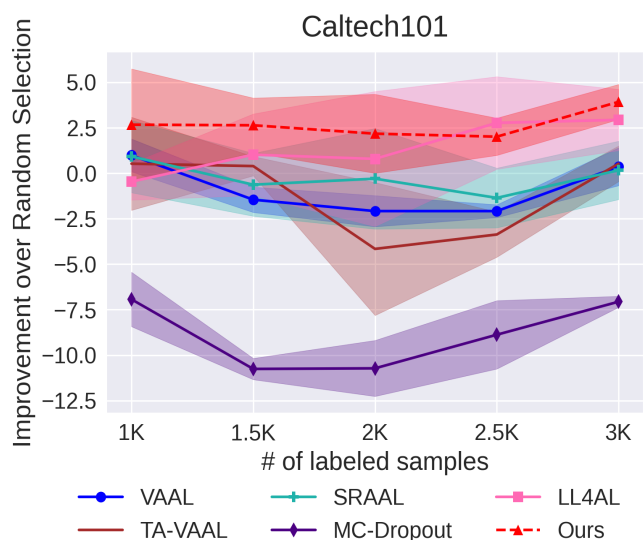


Figure 4: Mean accuracy improvements with standard deviations (shaded) of AL methods w.r.t random sampling over the number of labeled samples on Caltech101 dataset.

## 4.2 Active Learning on Imbalanced Datasets

**Datasets:** To evaluate the robustness of ADROIT, we test its performance on imbalanced datasets where class sample sizes significantly vary. We use two imbalanced datasets: (i) a Modified Imbalanced CIFAR10 and (ii) Caltech101 (Fei-Fei et al., 2006). In Modified Imbalanced CIFAR10, we randomly decrease sample sizes in the first five classes to introduce imbalance, with two ratios: 25 and 10. Caltech101 is inherently imbalanced, containing 8677 images distributed across 101 classes, with varying (32 – 800) samples per class. For Caltech101, we randomly select 1000 images with a 500 budget for subsequent iterations. For Modified CIFAR10, we follow the same approach as CIFAR10, as described in Section 4.1.

**Compared methods.** We evaluate the effectiveness of ADROIT in comparison to VAAL (Sinha et al., 2019), MC-Dropout (Gal et al., 2017), LL4AL (Yoo & Kweon, 2019), SRAAL (Zhang et al., 2020), TA-VAAL (Kim et al., 2021), and Random Selection. The model initialization and training undergoes the same procedures as described for balanced datasets in Section 4.1.

**Implementation details.** For the Modified imbalanced CIFAR10, we follow a similar implementation as described for CIFAR10 in Section 4.1. We use a classical ResNet-18 architecture for Caltech101. We utilize a Modified Wasserstein autoencoder (Tolstikhin et al., 2017) as the VAE and employ a 5-layer MLP as the discriminator. In both cases, we use the Adam optimizer (Kingma & Ba, 2014) (lr:  $5 \times 10^{-4}$ ). For more details, please refer to the appendix.

**Performance on modified CIFAR10.** Figure 3 illustrates the mean accuracy improvement with standard deviations relative to random sampling across various numbers of labeled samples on the modified CIFAR10 dataset. The dataset has two imbalance ratios, 10 (more imbalanced) and 25 (less imbalanced). ADROIT consistently outperforms all the other methods on both versions of modified imbalanced CIFAR10. For an imbalance ratio of 25, LL4AL follows as the second-best-performing AL approach. Meanwhile, in the case of an imbalance ratio of 10, SRAAL initially achieves the second-best accuracy; however, by the end, LL4AL surpasses SRAAL to become the second-best-performing AL approach. For absolute mean accuracy with standard deviations, refer to the appendix.

**Performance on Caltech101.** In Figure 4, we present the results for the various baselines along with the proposed model ADROIT on the highly imbalanced Caltech101 dataset. We show the metric mean accuracy improvement, along with standard deviations, in comparison to random sampling. We can observe that ADROIT consistently outperforms all other baseline methods by a significant margin. Initially, VAAL, SRAAL, and TA-VAAL achieve the second-highest accuracy; however, by the second iteration, their performance begins to decline. In contrast, LL4AL exhibits substantial improvement and ultimately emerges as the second-best performing AL method. MC-Dropout consistently performs the poorest among the compared baselines. For absolute mean accuracy values with standard deviations, please refer to the appendix.

## 4.3 Comparison of initialization methods in Active Learning

In this section, we explore different initialization strategies for the initial labeled pool selection in our AL method, ADROIT, and assess their impact. While many AL methods use random initialization, a practice that we also follow; we examine two other strategies: (i) *K*-center-based sampling, and (ii) *K*-means-based

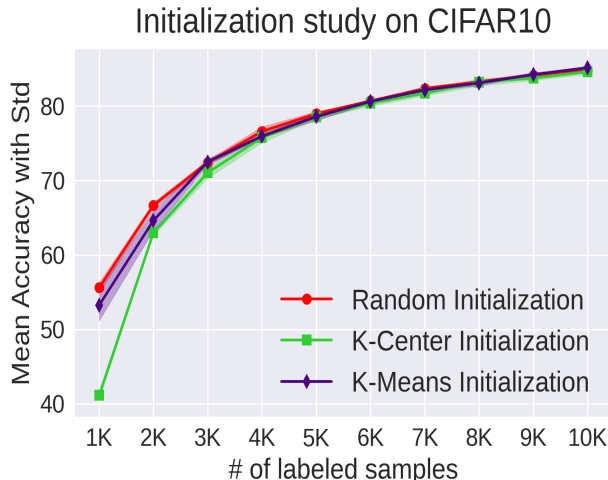


Figure 5: Comparison of initialization methods on the performance of ADROIT using (balanced) CIFAR10 dataset.

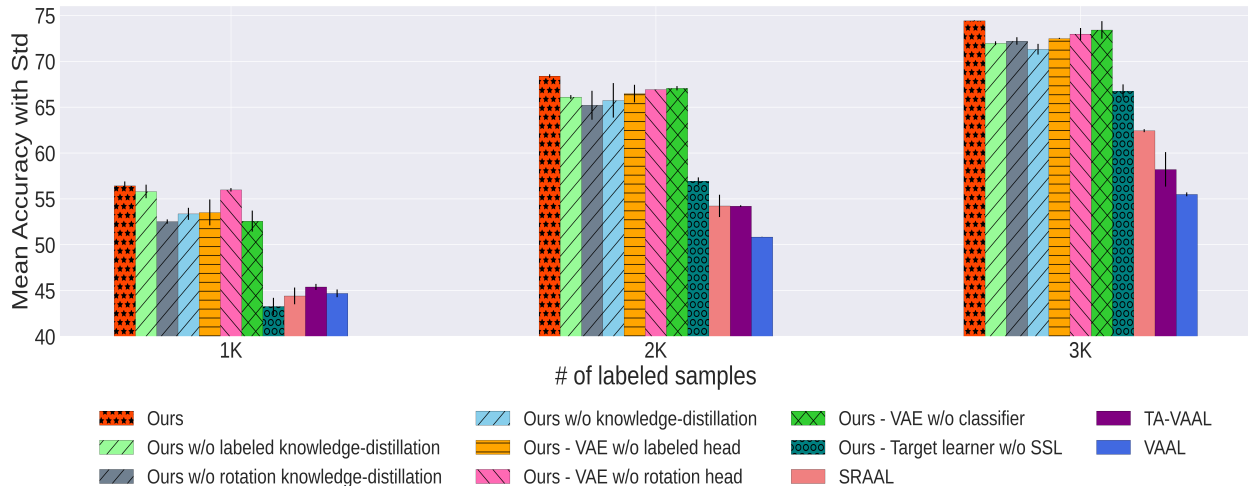


Figure 6: Results of ablation studies by selectively removing core components of ADROIT on (balanced) CIFAR10.

sampling. Figure 5 depicts ADROIT’s performance under these strategies. Random sampling shows the best initial performance, followed by  $K$ -means-based sampling, with  $K$ -center-based sampling exhibiting the poorest initial performance. Ultimately,  $K$ -means-based sampling achieves the highest accuracy, suggesting its potential as an alternative to random sampling.

## 5 Ablation

We perform ablation experiments on ADROIT, assessing the impact of key components. ADROIT crucially integrates teacher-student learning and applies self-supervised learning to unlabeled data. Evaluation includes scenarios with or without knowledge distillation and self-supervised learning. Additionally, we systematically modify the classifier and target learner. Figure 6 depicts ADROIT’s performance with or without key components on CIFAR10. ADROIT consistently outperforms variations, demonstrating the synergistic effectiveness of our proposed components in selecting informative unlabeled samples. Even ADROIT without specific components outperforms existing baselines.

## 6 Conclusion

This paper introduces *A Self-Supervised Framework for Learning Robust Representations for Active Learning* (ADROIT), a novel task-aware active learning framework. ADROIT leverages both labeled and unlabeled data to determine the most informative subset from the unlabeled pool. It establishes conditional relationships using labeled data through a proxy learner and enhances its performance through self-supervised learning on unlabeled data. Employing teacher-student learning between target and proxy learners ensures the proxy learner mimics the target-learner’s behavior. Empirical evidence across diverse datasets, including CIFAR10, CIFAR100, TinyImageNet-200, ImageNet-100, and Caltech101, consistently demonstrates ADROIT outperforming state-of-the-art active learning methods. Furthermore, our investigation into sampling strategies identifies  $K$ -means-based sampling as a promising alternative to random sampling. Ablation studies validate the significance of the proposed components in ADROIT.

## References

Sharat Agarwal, Himanshu Arora, Saket Anand, and Chetan Arora. Contextual diversity for active learning. In *Computer Vision—ECCV 2020: 16th European Conference, Glasgow, UK, August 23–28, 2020, Proceedings, Part XVI 16*, pp. 137–153. Springer, 2020.

- 
- Antreas Antoniou, Amos Storkey, and Harrison Edwards. Data augmentation generative adversarial networks. *arXiv preprint arXiv:1711.04340*, 2017.
- Hareesh Bahuleyan, Lili Mou, Olga Vechtomova, and Pascal Poupart. Variational attention for sequence-to-sequence models. *arXiv preprint arXiv:1712.08207*, 2017.
- Randall Balestriero, Mark Ibrahim, Vlad Sobal, Ari Morcos, Shashank Shekhar, Tom Goldstein, Florian Bordes, Adrien Bardes, Gregoire Mialon, Yuandong Tian, et al. A cookbook of self-supervised learning. *arXiv preprint arXiv:2304.12210*, 2023.
- William H Beluch, Tim Genewein, Andreas Nürnberger, and Jan M Köhler. The power of ensembles for active learning in image classification. In *Proceedings of the IEEE conference on computer vision and pattern recognition*, pp. 9368–9377, 2018.
- Vivien Cabannes, Leon Bottou, Yann Lecun, and Randall Balestriero. Active self-supervised learning: A few low-cost relationships are all you need. *arXiv preprint arXiv:2303.15256*, 2023.
- Francesco Calimeri, Aldo Marzullo, Claudio Stamile, and Giorgio Terracina. Biomedical data augmentation using generative adversarial neural networks. In *International conference on artificial neural networks*, pp. 626–634. Springer, 2017.
- Mathilde Caron, Hugo Touvron, Ishan Misra, Hervé Jégou, Julien Mairal, Piotr Bojanowski, and Armand Joulin. Emerging properties in self-supervised vision transformers. In *Proceedings of the IEEE/CVF international conference on computer vision*, pp. 9650–9660, 2021.
- Ting Chen, Simon Kornblith, Mohammad Norouzi, and Geoffrey Hinton. A simple framework for contrastive learning of visual representations. In *International conference on machine learning*, pp. 1597–1607. PMLR, 2020.
- Xi Chen, Yan Duan, Rein Houthoofd, John Schulman, Ilya Sutskever, and Pieter Abbeel. Infogan: Interpretable representation learning by information maximizing generative adversarial nets. *Advances in neural information processing systems*, 29, 2016a.
- Xi Chen, Diederik P Kingma, Tim Salimans, Yan Duan, Prafulla Dhariwal, John Schulman, Ilya Sutskever, and Pieter Abbeel. Variational lossy autoencoder. *arXiv preprint arXiv:1611.02731*, 2016b.
- Xinlei Chen and Kaiming He. Exploring simple siamese representation learning. In *Proceedings of the IEEE/CVF conference on computer vision and pattern recognition*, pp. 15750–15758, 2021.
- David Cohn, Les Atlas, and Richard Ladner. Improving generalization with active learning. *Machine learning*, 15:201–221, 1994.
- Corinna Cortes, Giulia DeSalvo, Mehryar Mohri, Ningshan Zhang, and Claudio Gentile. Active learning with disagreement graphs. In *International Conference on Machine Learning*, pp. 1379–1387. PMLR, 2019.
- Jia Deng, Wei Dong, Richard Socher, Li-Jia Li, Kai Li, and Li Fei-Fei. Imagenet: A large-scale hierarchical image database. In *2009 IEEE conference on computer vision and pattern recognition*, pp. 248–255. Ieee, 2009.
- Carl Doersch. Tutorial on variational autoencoders. *arXiv preprint arXiv:1606.05908*, 2016.
- Carl Doersch, Abhinav Gupta, and Alexei A Efros. Unsupervised visual representation learning by context prediction. In *Proceedings of the IEEE international conference on computer vision*, pp. 1422–1430, 2015.
- Chris Donahue, Zachary C Lipton, Akshay Balsubramani, and Julian McAuley. Semantically decomposing the latent spaces of generative adversarial networks. *arXiv preprint arXiv:1705.07904*, 2017.
- Jeff Donahue, Philipp Krähenbühl, and Trevor Darrell. Adversarial feature learning. *arXiv preprint arXiv:1605.09782*, 2016.

- 
- Sayna Ebrahimi, Anna Rohrbach, and Trevor Darrell. Gradient-free policy architecture search and adaptation. In *Conference on Robot Learning*, pp. 505–514. PMLR, 2017.
- Sayna Ebrahimi, William Gan, Dian Chen, Giscard Biamby, Kamyar Salahi, Michael Laielli, Shizhan Zhu, and Trevor Darrell. Minimax active learning. *arXiv preprint arXiv:2012.10467*, 2020.
- Li Fei-Fei, Robert Fergus, and Pietro Perona. One-shot learning of object categories. *IEEE transactions on pattern analysis and machine intelligence*, 28(4):594–611, 2006.
- Yarin Gal, Riashat Islam, and Zoubin Ghahramani. Deep bayesian active learning with image data. In *International conference on machine learning*, pp. 1183–1192. PMLR, 2017.
- Yaroslav Ganin and Victor Lempitsky. Unsupervised domain adaptation by backpropagation. In *International conference on machine learning*, pp. 1180–1189. PMLR, 2015.
- Mingfei Gao, Zizhao Zhang, Guo Yu, Sercan Ö Arık, Larry S Davis, and Tomas Pfister. Consistency-based semi-supervised active learning: Towards minimizing labeling cost. In *Computer Vision—ECCV 2020: 16th European Conference, Glasgow, UK, August 23–28, 2020, Proceedings, Part X 16*, pp. 510–526. Springer, 2020.
- Yonatan Geifman and Ran El-Yaniv. Deep active learning with a neural architecture search. *Advances in Neural Information Processing Systems*, 32, 2019.
- Spyros Gidaris, Praveer Singh, and Nikos Komodakis. Unsupervised representation learning by predicting image rotations. *arXiv preprint arXiv:1803.07728*, 2018.
- Ian Goodfellow, Jean Pouget-Abadie, Mehdi Mirza, Bing Xu, David Warde-Farley, Sherjil Ozair, Aaron Courville, and Yoshua Bengio. Generative adversarial nets. *Advances in neural information processing systems*, 27, 2014.
- Jifeng Guo, Zhiqi Pang, Miaoyuan Bai, Peijiao Xie, and Yu Chen. Dual generative adversarial active learning. *Applied Intelligence*, 51:5953–5964, 2021.
- Kaiming He, Xiangyu Zhang, Shaoqing Ren, and Jian Sun. Deep residual learning for image recognition. In *Proceedings of the IEEE conference on computer vision and pattern recognition*, pp. 770–778, 2016.
- Kaiming He, Xinlei Chen, Saining Xie, Yanghao Li, Piotr Dollár, and Ross Girshick. Masked autoencoders are scalable vision learners. In *Proceedings of the IEEE/CVF conference on computer vision and pattern recognition*, pp. 16000–16009, 2022.
- Geoffrey Hinton, Oriol Vinyals, and Jeff Dean. Distilling the knowledge in a neural network. *arXiv preprint arXiv:1503.02531*, 2015.
- Geoffrey E Hinton and Ruslan R Salakhutdinov. Reducing the dimensionality of data with neural networks. *science*, 313(5786):504–507, 2006.
- Geoffrey E Hinton, Alex Krizhevsky, and Sida D Wang. Transforming auto-encoders. In *Artificial Neural Networks and Machine Learning—ICANN 2011: 21st International Conference on Artificial Neural Networks, Espoo, Finland, June 14–17, 2011, Proceedings, Part I 21*, pp. 44–51. Springer, 2011.
- Neil Houlsby, Ferenc Huszár, Zoubin Ghahramani, and Máté Lengyel. Bayesian active learning for classification and preference learning. *arXiv preprint arXiv:1112.5745*, 2011.
- Sheng-Wei Huang, Che-Tsung Lin, Shu-Ping Chen, Yen-Yi Wu, Po-Hao Hsu, and Shang-Hong Lai. Auggan: Cross domain adaptation with gan-based data augmentation. In *Proceedings of the European Conference on Computer Vision (ECCV)*, pp. 718–731, 2018.
- Siyu Huang, Tianyang Wang, Haoyi Xiong, Jun Huan, and Dejing Dou. Semi-supervised active learning with temporal output discrepancy. In *Proceedings of the IEEE/CVF International Conference on Computer Vision*, pp. 3447–3456, 2021.

- 
- Xun Huang, Yixuan Li, Omid Poursaeed, John Hopcroft, and Serge Belongie. Stacked generative adversarial networks. In *Proceedings of the IEEE conference on computer vision and pattern recognition*, pp. 5077–5086, 2017.
- Juan Eugenio Iglesias, Ender Konukoglu, Albert Montillo, Zhuowen Tu, and Antonio Criminisi. Combining generative and discriminative models for semantic segmentation of ct scans via active learning. In *Information Processing in Medical Imaging: 22nd International Conference, IPMI 2011, Kloster Irsee, Germany, July 3-8, 2011. Proceedings 22*, pp. 25–36. Springer, 2011.
- Phillip Isola, Jun-Yan Zhu, Tinghui Zhou, and Alexei A Efros. Image-to-image translation with conditional adversarial networks. In *Proceedings of the IEEE conference on computer vision and pattern recognition*, pp. 1125–1134, 2017.
- Qiuye Jin, Mingzhi Yuan, Shiman Li, Haoran Wang, Manning Wang, and Zhijian Song. Cold-start active learning for image classification. *Information Sciences*, 616:16–36, 2022.
- Lukasz Kaiser, Samy Bengio, Aurko Roy, Ashish Vaswani, Niki Parmar, Jakob Uszkoreit, and Noam Shazeer. Fast decoding in sequence models using discrete latent variables. In *International Conference on Machine Learning*, pp. 2390–2399. PMLR, 2018.
- Kwanyoung Kim, Dongwon Park, Kwang In Kim, and Se Young Chun. Task-aware variational adversarial active learning. In *Proceedings of the IEEE/CVF Conference on Computer Vision and Pattern Recognition*, pp. 8166–8175, 2021.
- Diederik Kingma, Tim Salimans, Ben Poole, and Jonathan Ho. Variational diffusion models. *Advances in neural information processing systems*, 34:21696–21707, 2021.
- Diederik P Kingma and Jimmy Ba. Adam: A method for stochastic optimization. *arXiv preprint arXiv:1412.6980*, 2014.
- Diederik P Kingma and Max Welling. Auto-encoding variational bayes. *arXiv preprint arXiv:1312.6114*, 2013.
- Durk P Kingma, Shakir Mohamed, Danilo Jimenez Rezende, and Max Welling. Semi-supervised learning with deep generative models. *Advances in neural information processing systems*, 27, 2014.
- Durk P Kingma, Tim Salimans, Rafal Jozefowicz, Xi Chen, Ilya Sutskever, and Max Welling. Improved variational inference with inverse autoregressive flow. *Advances in neural information processing systems*, 29, 2016.
- Andreas Kirsch, Joost Van Amersfoort, and Yarin Gal. Batchbald: Efficient and diverse batch acquisition for deep bayesian active learning. *Advances in neural information processing systems*, 32, 2019.
- Alex Krizhevsky, Geoffrey Hinton, et al. Learning multiple layers of features from tiny images. 2009.
- Alex Krizhevsky, Ilya Sutskever, and Geoffrey E Hinton. Imagenet classification with deep convolutional neural networks. *Advances in neural information processing systems*, 25, 2012.
- Ya Le and Xuan Yang. Tiny imagenet visual recognition challenge. *CS 231N*, 7(7):3, 2015.
- Chunyuan Li, Jianwei Yang, Pengchuan Zhang, Mei Gao, Bin Xiao, Xiyang Dai, Lu Yuan, and Jianfeng Gao. Efficient self-supervised vision transformers for representation learning. *arXiv preprint arXiv:2106.09785*, 2021a.
- Minghan Li, Xialei Liu, Joost van de Weijer, and Bogdan Raducanu. Learning to rank for active learning: A listwise approach. In *2020 25th International Conference on Pattern Recognition (ICPR)*, pp. 5587–5594. IEEE, 2021b.
- Jianxin Lin, Yingce Xia, Tao Qin, Zhibo Chen, and Tie-Yan Liu. Conditional image-to-image translation. In *Proceedings of the IEEE conference on computer vision and pattern recognition*, pp. 5524–5532, 2018.

- 
- Calvin Luo. Understanding diffusion models: A unified perspective. *arXiv preprint arXiv:2208.11970*, 2022.
- Shuang Ma, Jianlong Fu, Chang Wen Chen, and Tao Mei. Da-gan: Instance-level image translation by deep attention generative adversarial networks. In *Proceedings of the IEEE conference on computer vision and pattern recognition*, pp. 5657–5666, 2018.
- Andrew McCallum, Kamal Nigam, et al. Employing em and pool-based active learning for text classification. In *ICML*, volume 98, pp. 350–358. Citeseer, 1998.
- Mehdi Mirza and Simon Osindero. Conditional generative adversarial nets. *arXiv preprint arXiv:1411.1784*, 2014.
- Shlok Mishra, Joshua Robinson, Huiwen Chang, David Jacobs, Aaron Sarna, Aaron Maschinot, and Dilip Krishnan. A simple, efficient and scalable contrastive masked autoencoder for learning visual representations. *arXiv preprint arXiv:2210.16870*, 2022.
- Ali Mottaghi and Serena Yeung. Adversarial representation active learning. *arXiv preprint arXiv:1912.09720*, 2019.
- Mehdi Noroozi and Paolo Favaro. Unsupervised learning of visual representations by solving jigsaw puzzles. In *European conference on computer vision*, pp. 69–84. Springer, 2016.
- Augustus Odena. Semi-supervised learning with generative adversarial networks. *arXiv preprint arXiv:1606.01583*, 2016.
- Alec Radford, Luke Metz, and Soumith Chintala. Unsupervised representation learning with deep convolutional generative adversarial networks. *arXiv preprint arXiv:1511.06434*, 2015.
- Ali Razavi, Aaron Van den Oord, and Oriol Vinyals. Generating diverse high-fidelity images with vq-vae-2. *Advances in neural information processing systems*, 32, 2019.
- Pengzhen Ren, Yun Xiao, Xiaojun Chang, Po-Yao Huang, Zhihui Li, Brij B Gupta, Xiaojiang Chen, and Xin Wang. A survey of deep active learning. *ACM computing surveys (CSUR)*, 54(9):1–40, 2021.
- Yassir Saquil, Kwang In Kim, and Peter Hall. Ranking cgans: Subjective control over semantic image attributes. *arXiv preprint arXiv:1804.04082*, 2018.
- Ozan Sener and Silvio Savarese. Active learning for convolutional neural networks: A core-set approach. *arXiv preprint arXiv:1708.00489*, 2017.
- H Sebastian Seung, Manfred Opper, and Haim Sompolinsky. Query by committee. In *Proceedings of the fifth annual workshop on Computational learning theory*, pp. 287–294, 1992.
- Changjian Shui, Fan Zhou, Christian Gagné, and Boyu Wang. Deep active learning: Unified and principled method for query and training. In *International Conference on Artificial Intelligence and Statistics*, pp. 1308–1318. PMLR, 2020.
- Samarth Sinha, Sayna Ebrahimi, and Trevor Darrell. Variational adversarial active learning. In *Proceedings of the IEEE/CVF International Conference on Computer Vision*, pp. 5972–5981, 2019.
- Ilya Tolstikhin, Olivier Bousquet, Sylvain Gelly, and Bernhard Schoelkopf. Wasserstein auto-encoders. *arXiv preprint arXiv:1711.01558*, 2017.
- Arash Vahdat and Jan Kautz. Nvae: A deep hierarchical variational autoencoder. *Advances in neural information processing systems*, 33:19667–19679, 2020.
- Shuo Wang, Yuexiang Li, Kai Ma, Ruhui Ma, Haibing Guan, and Yefeng Zheng. Dual adversarial network for deep active learning. In *Computer Vision—ECCV 2020: 16th European Conference, Glasgow, UK, August 23–28, 2020, Proceedings, Part XXIV 16*, pp. 680–696. Springer, 2020.

- 
- Zhendong Wang, Huangjie Zheng, Pengcheng He, Weizhu Chen, and Mingyuan Zhou. Diffusion-gan: Training gans with diffusion. *arXiv preprint arXiv:2206.02262*, 2022.
- Lilian Weng. From autoencoder to beta-vae. *lilianweng.github.io*, 2018. URL <https://lilianweng.github.io/posts/2018-08-12-vae/>.
- Lilian Weng. Self-supervised representation learning. *lilianweng.github.io*, 2019. URL <https://lilianweng.github.io/posts/2019-11-10-self-supervised/>.
- Haowen Xu, Wenxiao Chen, Nengwen Zhao, Zeyan Li, Jiahao Bu, Zhihan Li, Ying Liu, Youjian Zhao, Dan Pei, Yang Feng, et al. Unsupervised anomaly detection via variational auto-encoder for seasonal kpis in web applications. In *Proceedings of the 2018 world wide web conference*, pp. 187–196, 2018.
- Wilson Yan, Yunzhi Zhang, Pieter Abbeel, and Aravind Srinivas. Videogpt: Video generation using vq-vae and transformers. *arXiv preprint arXiv:2104.10157*, 2021.
- Donggeun Yoo and In So Kweon. Learning loss for active learning. In *Proceedings of the IEEE/CVF conference on computer vision and pattern recognition*, pp. 93–102, 2019.
- Xueying Zhan, Qingzhong Wang, Kuan-hao Huang, Haoyi Xiong, Dejing Dou, and Antoni B Chan. A comparative survey of deep active learning. *arXiv preprint arXiv:2203.13450*, 2022.
- Beichen Zhang, Liang Li, Shijie Yang, Shuhui Wang, Zheng-Jun Zha, and Qingming Huang. State-relabeling adversarial active learning. In *Proceedings of the IEEE/CVF conference on computer vision and pattern recognition*, pp. 8756–8765, 2020.
- Zicheng Zhang, Yinglu Liu, Congying Han, Tiande Guo, Ting Yao, and Tao Mei. Generalized one-shot domain adaptation of generative adversarial networks. *Advances in Neural Information processing systems*, 35:13718–13730, 2022.
- Jia-Jie Zhu and José Bento. Generative adversarial active learning. *arXiv preprint arXiv:1702.07956*, 2017.
- Jun-Yan Zhu, Taesung Park, Phillip Isola, and Alexei A Efros. Unpaired image-to-image translation using cycle-consistent adversarial networks. In *Proceedings of the IEEE international conference on computer vision*, pp. 2223–2232, 2017a.
- Xinyue Zhu, Yifan Liu, Zengchang Qin, and Jiahong Li. Data augmentation in emotion classification using generative adversarial networks. *arXiv preprint arXiv:1711.00648*, 2017b.

---

## A Additional Results: Active Learning on Imbalanced Datasets

Figures 3 and 4 in the main paper, show the performance improvement (mean accuracy with standard deviation) relative to Random sampling over the number of labeled samples on modified CIFAR10 and Caltech101 respectively. In this section, we provide the absolute accuracy curves over the number of labeled samples on modified CIFAR10 and Caltech101 in Figure 7 and 8 respectively.

## B ImageNet-100

In this paper, we employed a subset of ImageNet-1K (ILSVRC-2012) Deng et al. (2009), comprising randomly selected 100 classes. To facilitate a thorough investigation, we have provided the list of these 100 classes utilized for assessing the performance of the active learning baselines in our experiments, as detailed in Table1.

## C Additional Ablation on CIFAR100

In addition to the ablation study presented in Section 5, we also perform an ablation experiment on ADROIT utilizing the (balanced) CIFAR-100 dataset. This experiment assesses the impact of self-supervised learning, implemented by predicting the random transformations (Figure ??) applied to the unlabeled samples, on the overall model performance.

Figure 9 demonstrates the performance of ADROIT with or without applying self-supervised learning on the target task learner in comparison to existing active learning baselines. It can be seen that ADROIT with all the proposed components, including self-supervised loss on the target task learner, achieves the best performance compared to the existing active learning baselines. However, ADROIT without using self-supervision in target task learner training performs slightly worse compared to the existing active learning baselines. This highlights the importance of self-supervised learning in the overall model performance and the significance of exploiting the freely available abundant pool of unlabeled samples to achieve the best overall model performance. As future work, we will explore the effects of utilizing unlabeled samples in active learning model performance through various self-supervised and semi-supervised approaches.

## D Details on hyperparameters

Table 2 shows the hyperparameters that we use to train our proposed model (ADROIT). We set these hyperparameters following VAAL Sinha et al. (2019) and SRAAL Zhang et al. (2020) settings.

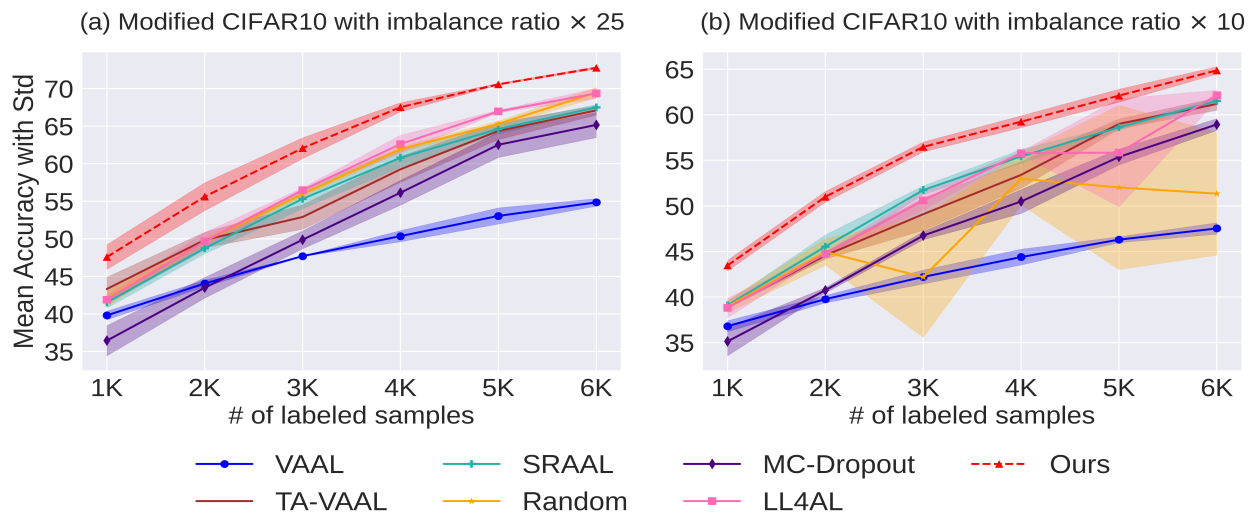


Figure 7: Mean accuracy with standard deviations (shaded) of AL methods over the number of labeled samples on modified imbalanced CIFAR10 dataset.

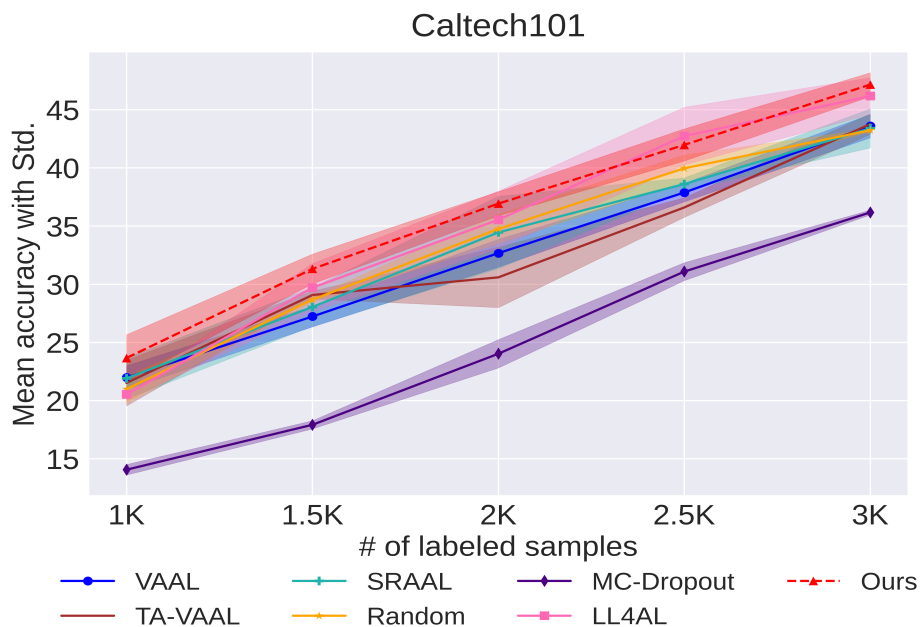


Figure 8: Mean accuracy with standard deviations (shaded) of AL methods over the number of labeled samples on Caltech101 dataset.

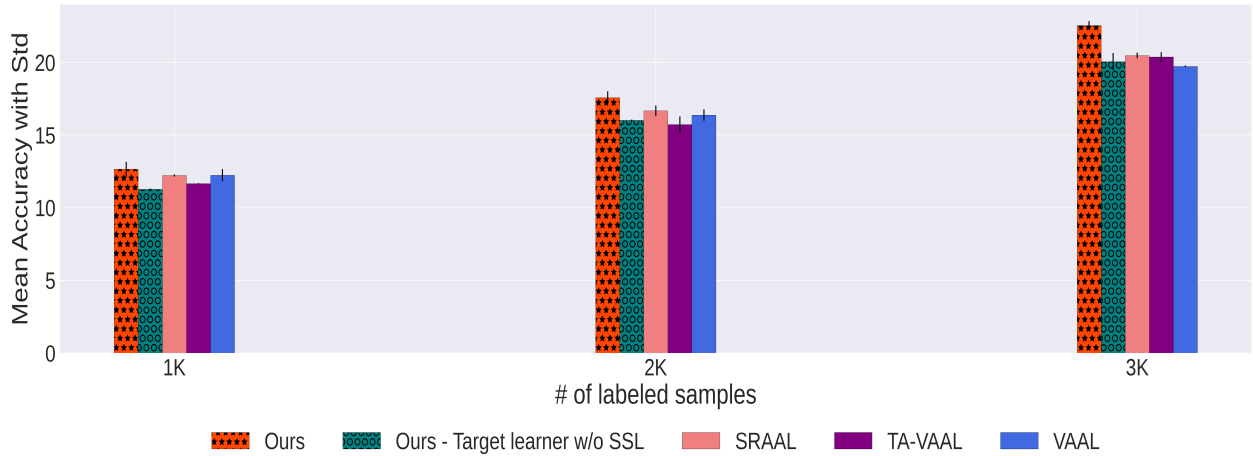


Figure 9: Results of ablation study comparing the performance of ADROIT with or without using self-supervised learning in target task-learner training on (balanced) CIFAR100.

Table 1: The list of classes from ImageNet-100, which are randomly chosen from the original ImageNet-1K (ILSVRC-2012).

List Of ImageNet-100 Classes			
n01632777	n01667114	n01744401	n01753488
n01768244	n01770081	n01798484	n01829413
n01843065	n01871265	n01872401	n01981276
n02006656	n02012849	n02025239	n02085620
n02086079	n02089867	n02091831	n02094258
n02096294	n02100236	n02100877	n02102040
n02105251	n02106550	n02110627	n02120079
n02130308	n02168699	n02169497	n02177972
n02264363	n02417914	n02422699	n02437616
n02483708	n02488291	n02489166	n02494079
n02504013	n02667093	n02687172	n02788148
n02791124	n02794156	n02814860	n02859443
n02895154	n02910353	n03000247	n03208938
n03223299	n03271574	n03291819	n03347037
n03445777	n03529860	n03530642	n03602883
n03627232	n03649909	n03666591	n03761084
n03770439	n03773504	n03788195	n03825788
n03866082	n03877845	n03908618	n03916031
n03929855	n03954731	n04009552	n04019541
n04141327	n04147183	n04235860	n04285008
n04286575	n04328186	n04347754	n04355338
n04423845	n04442312	n04456115	n04485082
n04486054	n04505470	n04525038	n07248320
n07716906	n07730033	n07768694	n07836838
n07860988	n07871810	n11939491	n12267677

Table 2: Hyperparameters used in ADROIT.  $d$  denotes the dimension of the latent space of the VAE.  $\alpha_1, \alpha_2$  and  $\alpha_3$  are the learning rates of VAE, Discriminator and Target task-learner respectively.  $\lambda_1, \lambda_2, \lambda_3$  and  $\lambda_4$  are the regularization hyperparameters that determine the effect of various components in learning an effective latent space representation using VAE, used in Eq. (7).  $\beta$  is the Lagrangian parameter used in Eq. (1). ‘initial’ denotes the size of initial labeled pool. ‘budget’ denotes the number of unlabeled samples selected in the subsequent iterations.

Dataset	Hyperparameters												
	$d$	$\alpha_1$	$\alpha_2$	$\alpha_3$	$\lambda_1$	$\lambda_2$	$\lambda_3$	$\lambda_4$	$\beta$	epochs	batch-size	initial / budget	image-size
CIFAR10 Krizhevsky et al. (2009)	32	$5 \times 10^{-4}$	$5 \times 10^{-4}$	$1 \times 10^{-2}$	1	$5 \times 10^{-1}$	$5 \times 10^{-1}$	1	1	100	128	1000/1000	$32 \times 32$
CIFAR100 Krizhevsky et al. (2009)	32	$5 \times 10^{-4}$	$5 \times 10^{-4}$	$1 \times 10^{-2}$	1	$5 \times 10^{-1}$	$5 \times 10^{-1}$	1	1	100	128	1000/1000	$32 \times 32$
TinyImageNet-200 Le & Yang (2015)	32	$5 \times 10^{-4}$	$5 \times 10^{-4}$	$1 \times 10^{-2}$	1	$5 \times 10^{-1}$	$5 \times 10^{-1}$	1	1	100	128	2000/2000	$64 \times 64$
ImageNet-100 Deng et al. (2009)	128	$5 \times 10^{-4}$	$5 \times 10^{-4}$	$1 \times 10^{-2}$	1	$5 \times 10^{-1}$	$5 \times 10^{-1}$	1	1	100	32	2000/2000	$224 \times 224$
Modified Imbalanced CIFAR10	32	$5 \times 10^{-4}$	$5 \times 10^{-4}$	$1 \times 10^{-2}$	1	$5 \times 10^{-1}$	$5 \times 10^{-1}$	1	1	100	128	1000/1000	$32 \times 32$
Caltech101 Fei-Fei et al. (2006)	128	$5 \times 10^{-4}$	$5 \times 10^{-4}$	$1 \times 10^{-2}$	1	$5 \times 10^{-1}$	$5 \times 10^{-1}$	1	1	100	32	1000/500	$224 \times 224$